Magnon spin transport driven by the spin chemical potential in Permalloy

Hanfeng Wang
MIT EECS
hanfengw@mit.edu

Dimple Kochar
MIT EECS
dkochar@mit.edu

Zhongqiang Hu
MIT EECS
zhongqhu@mit.edu

***Abstract*—Spin transport properties is of great significance in developing magnon-based devices [1] and spintronics networks [2], which have been studied in several systems such as magnetic insulator [3]–[5] and metals [6]. Specifically, in this project, we explore both the dynamical and steady-state spin potential distribution in Permalloy, a kind of magnetic metal, in response to spin injection on the boundary. We model the spin transport and spin leakage using two kinds of spin resistors, model the spin accumulation using a spin capacitor, and then construct an tractable circuit diagram, in which we can make use of the knowledge of simulation methods introduced in the class.**

I. Introduction & Motivations

A spintronics network propagates the information encoded in spin degree of freedom. Transmission loss is always a limit in different kinds of networks [7], [8]. In this project, we focus on the spin current transport containing diffusion and damping in Permalloy, a kind of ferromagnetic conductor [9], [10]. We want to consider about a magnetic waveguide modeled by a 1D geometry shown in Fig. 1(a) or a 2D geometry to model it more precisely (will add later). The structure contains two Platinum strips deposited on both sides of a Permalloy bar. One Platinum strip acts as an injector, where the spin current is generated due to Spin Hall Effect (SHE). SHE injects spins with a specific direction, changing the chemical potential of magnon, a quasi-particle represents the collective excitation of the electrons' spin structure in a crystal lattice. Magnon will then diffuse and damp in permalloy. The other one acts as a detector, where the spin current is transformed to charge current due to inverse Spin Hall Effect (ISHE). Here, the spin current transport within Permalloy is governed by the diffusion equation and the Helmholtz-type equation [1]:

$$\frac{2e}{\hbar}\boldsymbol{j}_\mathrm{s} = -\sigma_\mathrm{e}\nabla\mu_\mathrm{s} \qquad \nabla^2\mu_\mathrm{s} = \frac{\mu_\mathrm{s}}{\ell_\mathrm{sf}^2} \tag{1}$$

where $\boldsymbol{j}_\mathrm{s}$ is the spin current, μ_s is the spin chemical potential, and other parameters are associated with the properties of Permalloy. In Fig. 1(b), we show the the equivalent circuit diagram of the one-dimensional (1D) spin current transport model (higher dimensions will be discussed in the following work), where node $0'$ and N represents the Platinum/Permalloy interface of the injector and detector. In our network, we make the discretization on the Permalloy bar and get nodes $1, 2, ..., N$, and each of them is associated with a spin chemical potential μ_i. Two neighboring nodes are connected through a spin resistor R_1, as well as a spin capacitor originated from the spin-accumulation effect. Besides, each node is also connected with ground through a resistor R_2, which represents the damping, i.e., spin leakage.

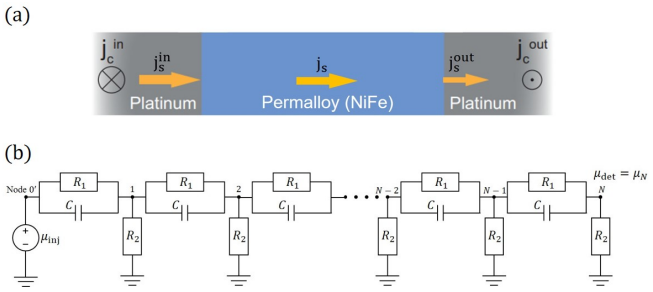

Fig. 1. (a) Spin current transport in Platinum/Permalloy/Platinum heterostructure [4]. (b) Equivalent circuit diagram for the spin current model.

II. Problem formulation

The state of our system is spin chemical potential μ_i on each node. Here we use x_i to substitute all of them, where:

$$\boldsymbol{x} = [\mu_1, \mu_2, ..., \mu_N]^T \tag{2}$$

The parameters we need are [9], [10]: $\hbar = 1.05 \times 10^{-34}$ J $\cdot$ s, $e = 1.6 \times 10^{-19}$ C, $\Delta L = L/N$ is the distance between two neighboring nodes, $\rho_\mathrm{e} = 2.3 \times 10^{-8}$ $\Omega \cdot$ m is the charge resistivity, $\ell_\mathrm{sf} = 4.5 \times 10^{-9}$ m is the spin diffusion length, and $\tau_\mathrm{sf} = 4.0 \times 10^{-11}$ s is the spin relaxation time (all values at room temperature 300 K). Here we set:

$$\boldsymbol{p} = [\hbar, e, L, N, \rho_\mathrm{e}, T, \ell_\mathrm{sf}, \tau_\mathrm{sf}]^T \tag{3}$$

Multiple sources can be considered in our system. However, to make the problem clear, we only consider about one source. Therefore, our source vector is:

$$\boldsymbol{u} = [u_\mathrm{inj}, 0, ..., 0]^T \tag{4}$$

In time domain, at a specific time t_0 Our final set of equations that describe entirely the problem is:

$$\frac{d\boldsymbol{x}}{dt} = (\mathbf{I} - \mathbf{C})^{-1}(\mathbf{A}\boldsymbol{x} + \mathbf{B}\boldsymbol{u}) \tag{5}$$

where:

$$\mathbf{A} = \frac{1}{C}\begin{bmatrix} R' & R'' & 0 & \cdots & 0 & 0 & 0 \\ R'' & R' & R'' & \cdots & 0 & 0 & 0 \\ 0 & R'' & R' & \cdots & 0 & 0 & 0 \\ \vdots & \vdots & \vdots & \ddots & \vdots & \vdots & \vdots \\ 0 & 0 & 0 & \cdots & R' & R'' & 0 \\ 0 & 0 & 0 & \cdots & R'' & R' & R'' \\ 0 & 0 & 0 & \cdots & 0 & 2R'' & 2(R'+R'') \end{bmatrix} \tag{6}$$

$$\mathbf{B} = \left[\frac{1}{2CR_1}, 0, 0, ..., 0, 0\right]^T \tag{7}$$

$$\mathbf{C} = \begin{bmatrix} 0 & \frac{1}{2} & 0 & \cdots & 0 & 0 & 0 \\ \frac{1}{2} & 0 & \frac{1}{2} & \cdots & 0 & 0 & 0 \\ 0 & \frac{1}{2} & 0 & \cdots & 0 & 0 & 0 \\ \vdots & \vdots & \vdots & \ddots & \vdots & \vdots & \vdots \\ 0 & 0 & 0 & \cdots & 0 & \frac{1}{2} & 0 \\ 0 & 0 & 0 & \cdots & \frac{1}{2} & 0 & \frac{1}{2} \\ 0 & 0 & 0 & \cdots & 0 & 1 & 0 \end{bmatrix} \tag{8}$$

Here $R_1 = 4e\rho_e\Delta L/\hbar$ the diffusion-related resistance, $R_2 = 4e\rho_e\ell_{sf}^2/\hbar\Delta L$ the damping-related resistance, $C = \hbar\tau_{sf}/4e\rho_e\Delta L$, $R' = -1/R_1 - 1/2R_2$, $R'' = 1/2R_1$.

The quantities of interest we care to observe is the chemical distribution:

$$\boldsymbol{y_1} = [\mu_1, \mu_2, ..., \mu_N]^T \tag{9}$$

III. Fundamental Numerical Methods

For the time dynamics, we utilized the Forward Euler method as well as the trapezoidal method with fixed time steps and logarithmic stepping. We ended up using the latter two for our results and the pseudo code for these two methods are shown in Algorithms 1 and 2 respectively. Note that no inverse were computed directly and MATLAB's \ was used wherever inverse is shown in the pseudo code.

IV. The Technical Challenge

When using Gradient Conjugate Residual (GCR) method to calculate static case in our model. Convergence preconditioners can be used to decrease the number of iteration times, making calculation more efficient. Here we show two preconditioners. The first one is Jacobi preconditioner or diagonal preconditioner, the other one is a kind of sparse preconditioner. Here we choose the tridiagonal part of matrix A as $\tilde{A}$. Then the GCR method is applied to make the calculation. The pseudocode is shown in Algorithm 3.

V. Results

In Fig. 2, we run a fixed time trapezoidal method with a time step of 1e-18 and show the distribution of the chemical potential across a 2D permalloy at 6 different time steps, with the final being the steady state result. In order to check for plausibility of our result, we compare with the result published in [1] as shown in Fig. 3. The distribution of steady state shown is similar to what we see although the material used is an insulator, which is different from our permalloy.

Algorithm 1 Dynamics using trapezoidal solver for linear system with fixed time step

Require: N: number of nodes; t_s: start time; t_e: end time; dt: time step; p: parameter vector; u: μ_{inj} input
  function COMPUTE_A_B(N, p)
    return A, b (as discussed in Section III)
  end function
  function EVALF(x, A, b)
    $f = Ax + bu$
    return f
  end function
  $J = I - A\Delta t/2$
  [L, U, P] = LU decomposition of J
  function TRAPEZOIDAL($evalf, \Delta t, N, u, A, b, L, U, P, t_s, t_e$)
    $t = t_s$
    $j = 1$
    x_i = null vector of size N
    repeat
      $\Gamma = x_i + (\Delta t * (evalf(x, A, b) + (b * u))/2)$
      $y = L^{-1}(P * \Gamma)$
      $x_i = U^{-1}y$
      $\psi(j) = x_i$
      $j = j + 1$
      $t = t + \Delta t$
    until $t > t_e$
    return ψ
  end function

Another way to verify if our circuit model is working fine is to simulate a smaller model on an online circuit simulator and check if the results we are getting match those. Fig. 4(c) shows the circuit simulated is a small 5x5 grid. Figs. 4(a) and (b) compare the results for $\mu_{\text{inj}} = 87$ kV. (The μ_{inj} is high as the online simulator outputs 0 for any voltage below 1 nV. It also shows the robustness of our model, that it can work over a very large range of μ_{inj}). Fig. 4(d) plots the % error at each node which is less than 0.4% everywhere, verifying the correctness of our code.

Logarithmic time steps are useful in our simulation as our dynamics change fast initially and move to a steady state. Having a small fixed step takes longer too. The same time range as before is run but with 2.5% of the number of steps that fixed time step of 10^{-17} s took. Here, our steps are spaced logarithmically. We see about 70% decrease in the simulation time (4.54 s for fixed at 10^{-17} s vs 2.61 s). In Fig. 5, we compare the error of the logarithmic stpping with a reference solution of fixed step with 10^{-18} s. For the earlier part, the error is larger, and it goes down as we go to steady state. We conclude that to obtain a fast visualization, where the user is alright with a 10% error, logarithmic time stepping can be used.

The effect of convergence preconditioners are shown in Fig. 6, from which we can see the Jacobi preconditioner is not efficient but the sparse preconditioner we chooose is much more efficient and can improve the number of iterations by a

Algorithm 2 Dynamics using trapezoidal solver for linear system with logarithmic time step

Require: N: number of nodes; t_s: start time; t_s: end time; p: parameter vector; u: μ_{inj} input
  function COMPUTE_A_B(N, p)
    return A, b (as discussed in Section III)
  end function
  function EVALF(x, A, b)
    $f = Ax + bu$
    return f
  end function
  function TRAPEZOIDAL($evalf, \Delta t_i, N, u, A, b, t_s, t_e$)
    $tt = [t_s, t_e]$ divided in logarithmic intervals
    $j = 1$
    $t = t_s$
    x_i = null vector of size N
    repeat
      $\Delta t = tt(j+1) - tt(j)$
      $\Gamma = x_i + (\Delta t * (evalf(x, A, b) + (b * u))/2)$
      $x_i = (I - A\Delta t/2)^{-1}\Gamma$
      $\psi(j) = x_i$
      $j = j + 1$
      $t = tt(j)$
    until $t > t_e$
    return ψ
  end function

Algorithm 3 Sparse Preconditioner

Require: A, b
  function TGCR_PRECOND($A, b, \text{tol}, \text{maxiters}$)
    $\tilde{A} \leftarrow$ Tridiagonal(A)
    [$\tilde{L}$,$\tilde{U}$,Perm] $\leftarrow$ lu($\tilde{A}$)
    $r = \tilde{U}\backslash(\tilde{L}\backslash(\text{Perm} \times b))$
    repeat
      $k \leftarrow k + 1$
      $p(:, k) = r$
      $Ap(:, k) = \tilde{U}\backslash(\tilde{L}\backslash(\text{Perm} \times A \times p(:, k)))$
      if $k > 1$ **then**
        repeat
          $\beta = Ap(:, k)' \times Ap(:, j)$
          $p(:, k) = p(:, k) - \beta \times p(:, j)$
          $Ap(:, k) = Ap(:, k) - \beta \times Ap(:, j)$
          $j = j + 1$
        until $j > k$
      end if
      $\text{norm\_}Ap = \text{norm}(Ap(:, k), 2)$
      $Ap(:, k) = Ap(:, k)/\text{norm\_}Ap$
      $p(:, k) = p(:, k)/\text{norm\_}Ap$
      $\alpha = r' \times Ap(:, k)$
      $x = x + \alpha \times p(:, k)$
      $r = r - \alpha \times Ap(:, k)$
      $r_n(k+1) = \text{norm}(r, 2)$
    until $r_n(k+1)/r_n(1) < tol$ or k $>$ maxiters
    return x, k
  end function

factor of 6.

VI. Technical Discussion

From Fig. 2, we found the total time to make the system stable is only $10^{-12}s$, meaning that it is very easy to be stable for our system. It is very important when we want to use it to transfer information. Unfortunately, the loss in Permalloy is a little bit large because of damping. One way to make it better is do it with low temperature.

VII. Ethics & Limitations

The calculation results of spin transport properties in this project might benefit quantum engineers and circuit engineers. For quantum engineers, they have a better understanding of the spin transport behavior in the ferromagnetic conductors and can therefore better manipulate spin currents to realize the transmission of quantum information. For circuit engineers, they have a better understanding of the advantages of spintronic devices compared with the conventional charge-based electronics, and will therefore pay attention to design spin-based circuits or neural networks.

Understanding the fundamental limitations is also important to determine whether the spin current transport mentioned in this project suitable for a certain application. The first important thing to note is that the numerical results presented are highly dependent on the parameters such as ℓ_{sf} and L, as shown in PM2. Due to this, no methods have been implemented to check if the results of the model quantitatively reflect the real case. Until now, compared with the existing experimental results, we can only make sure our calculation results are qualitatively correct. Second, our model approximates spin accumulation as spin capacitors which is not 100% accurate, since this approximation only applies to the case where the totally length of the bar L is in the same level of order as ℓ_{sf}. Third, regarding the physical structure, we assume Permalloy is uniform everywhere by taking the same parameters at every node. This material homogeneity assumption is not always perfect in reality, and the slight change of local parameters might lead to significant impacts. Fourth, since magnons carries not only spin momenta but also heat/energy flows, there are heat transfer effects which we are not considering and might interact with the spin transfer phenomenon.

VIII. Conclusions

In this project, we explore the spin transport properties in Permalloy by numerically calculating the spin potential distribution. We model the process of spin current transport by using two types of spin resistors to represent the spin transport process and spin leakage effect respectively, and also use one type of spin capacitor to represent the spin accumulation effect that introduces dynamics. Compared with the existing published results, our calculation qualitatively shows great

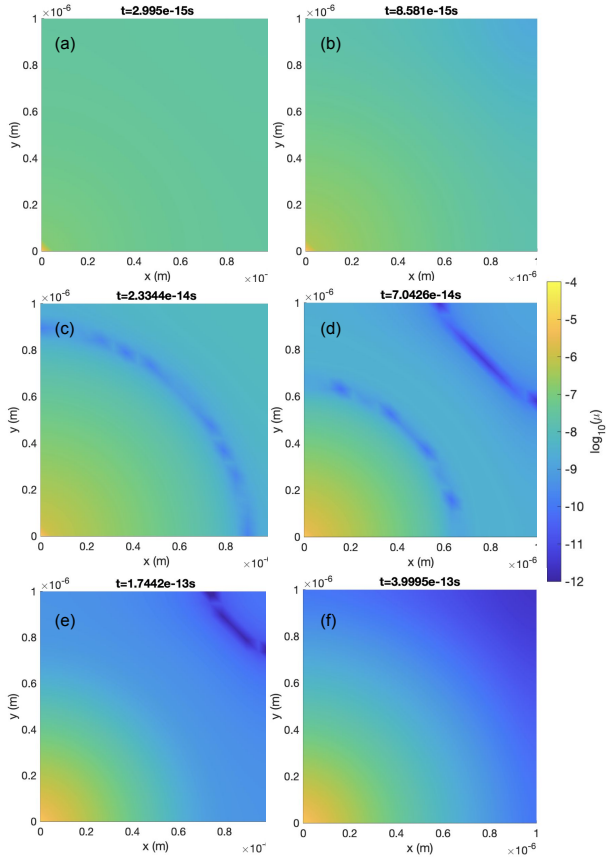

Fig. 2. The spin potential (μ) distribution across the 2D permalloy is shown at 6 different time steps with (f) being the steady state for a 20x20 grid with $\mu_{\text{inj}} = 8.7\mu V$

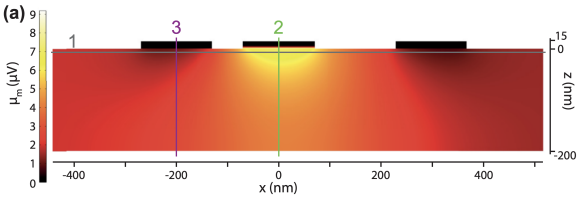

Fig. 3. This, plot taken from [1], shows distribution of the steady state similar to what we see from our simulation. Although their material is an insulator, (different from our permalloy), this shows our model is plausible.

consistency. We utilize the numerical techniques presented in the class, such as using GCR to calculated the steady state, using Jacobi/diagonal preconditioner to decrease the number of iterations, and using Trapezoidal to simulate the dynamic process. We believe our project is a good demonstration for the various numerical techniques, and will also benefit quantum engineers and circuit engineers who would like to make use of spin currents to transport information and energy.

REFERENCES

[1] A. V. Chumak, V. I. Vasyuchka, A. A. Serga, and B. Hillebrands, "Magnon spintronics," *Nature Physics*, vol. 11, no. 6, pp. 453–461,

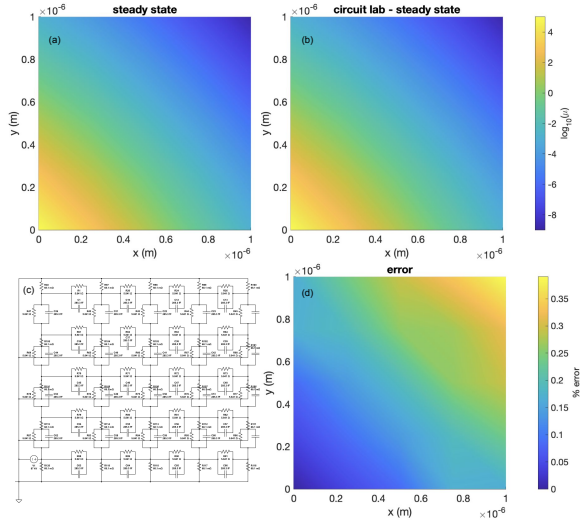

Fig. 4. A 5x5 grid using an online circuit simulator [11] as shown in (c), and steady state is obtained from it for $\mu_{\text{inj}} = 87kV$ and plotted in (b). Running the same simulation with our code, (a) is obtained. On comparing with (b), (d) plots the % error at each node which is less than 0.4% everywhere, verifying the correctness of our code.

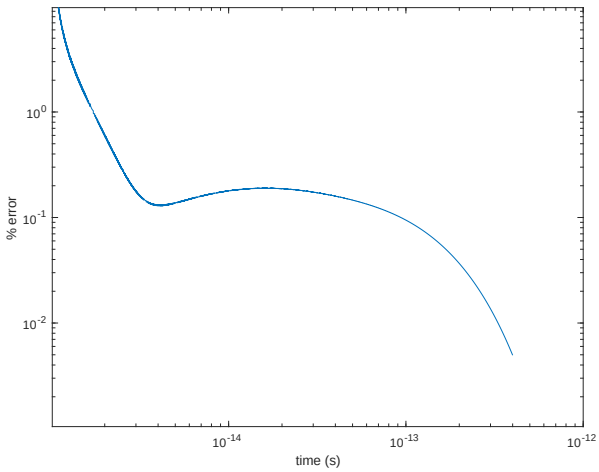

Fig. 5. Trapezoidal, run with a fixed time step of 10^{-18}, is our reference correct answer. Here, for the earlier part, the error is larger, and it goes down as we go to steady state. We conclude that to obtain a fast visualization where the user is alright with a 10% error, logarithmic time stepping can be used

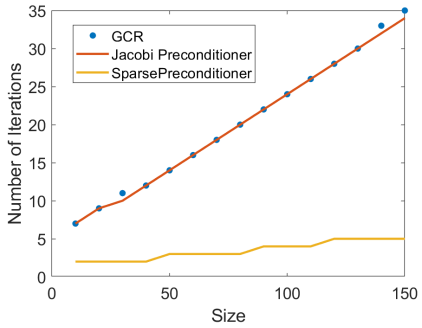

Fig. 6. Number of iterations with or without preconditioners. The Jacobi Preconditioner is not very efficient but the Sparse Preconditioner can improve the number of iterations by a factor of 6.

2015. [Online]. Available: https://doi.org/10.1038/nphys3347
[2] F. C. Langbein, S. Schirmer, and E. Jonckheere, "Time optimal information transfer in spintronics networks," in *2015 54th IEEE Conference on Decision and Control (CDC)*. IEEE, 2015, pp. 6454–6459. [Online]. Available: https://doi.org/10.1109/CDC.2015.7403236
[3] L. Cornelissen, J. Liu, R. Duine, J. B. Youssef, and B. Van Wees, "Long-distance transport of magnon spin information in a magnetic insulator at room temperature," *Nature Physics*, vol. 11, no. 12, pp. 1022–1026, 2015. [Online]. Available: https://doi.org/10.1038/nphys3465
[4] L. J. Cornelissen, K. J. H. Peters, G. E. W. Bauer, R. A. Duine, and B. J. van Wees, "Magnon spin transport driven by the magnon chemical potential in a magnetic insulator," *Phys. Rev. B*, vol. 94, p. 014412, Jul 2016. [Online]. Available: https://link.aps.org/doi/10.1103/PhysRevB.94.014412
[5] L. J. Cornelissen, J. Liu, B. J. van Wees, and R. A. Duine, "Spin-current-controlled modulation of the magnon spin conductance in a three-terminal magnon transistor," *Phys. Rev. Lett.*, vol. 120, p. 097702, Mar 2018. [Online]. Available: https://link.aps.org/doi/10.1103/PhysRevLett.120.097702
[6] M. Johnson and R. H. Silsbee, "Interfacial charge-spin coupling: Injection and detection of spin magnetization in metals," *Phys. Rev. Lett.*, vol. 55, pp. 1790–1793, Oct 1985. [Online]. Available: https://link.aps.org/doi/10.1103/PhysRevLett.55.1790
[7] Y. Lee, E. Bersin, A. Dahlberg, S. Wehner, and D. Englund, "A quantum router architecture for high-fidelity entanglement flows in quantum networks," *arXiv:2005.01852*, 2020. [Online]. Available: https://arxiv.org/abs/2005.01852
[8] P. C. Humphreys, N. Kalb, J. P. Morits, R. N. Schouten, R. F. Vermeulen, D. J. Twitchen, M. Markham, and R. Hanson, "Deterministic delivery of remote entanglement on a quantum network," *Nature*, vol. 558, no. 7709, pp. 268–273, 2018. [Online]. Available: https://doi.org/10.1038/s41586-018-0200-5
[9] E. Sagasta, Y. Omori, M. Isasa, Y. Otani, L. E. Hueso, and F. Casanova, "Spin diffusion length of permalloy using spin absorption in lateral spin valves," *Applied Physics Letters*, vol. 111, no. 8, p. 082407, 2017. [Online]. Available: https://doi.org/10.1063/1.4990652
[10] Y.-H. Zhu, X.-X. Zhang, J. Liu, and P.-S. He, "Spin-accumulation capacitance and its application to magnetoimpedance," *Journal of Applied Physics*, vol. 122, no. 4, p. 043902, 2017. [Online]. Available: https://doi.org/10.1063/1.4995289
[11] [Online]. Available: https://www.circuitlab.com/